

Article

Analysis of Combustion Conditions for Sustainable Dual-Fuel Mixtures

Michal Puškár¹, Jozef Živčák¹, Matúš Lavčák^{1,*}, Marieta Šoltésová² and Melichar Kopas¹¹ Faculty of Mechanical Engineering, TU Košice, Letná 9, 040 01 Košice, Slovakia² Faculty of Mining, Ecology, Process Control and Geotechnology, TU Košice, Park Komenského 19, 040 01 Košice, Slovakia

* Correspondence: matus.lavcak@tuke.sk

Abstract: The scientific contribution is focused on the analysis and optimization of combustion conditions concerning the dual-fuel mixtures. The greatest attention was paid to the temperature of intake air when a mixture of ethanol and gasoline created the applied fuel. An experimental fuel mixture was added into the intake pipe and ultra-low sulphur diesel fuel (ULSDF) was added directly into the engine cylinder using the CR (common rail) injection system. The article analysed the medium- and high-level operational engine load, whereby the engine timing parameters originally corresponded to a conventional diesel engine. The obtained results of the performed analysis showed that the temperature of intake air affected the following operational parameters: delay of ignition, pressure rise rate in the engine cylinder and the maximum level of pressure in the engine cylinder. Lower values of the intake air temperature enabled higher injection speeds for the ethanol-sustainable mixture (ESM), especially at high engine loads. An increase in the injection speed was possible due to lower charge air temperature. While there were reduced nitrogen oxide emissions, we also noted a reduction in both carbon monoxide emissions and the total amount of unburned hydrocarbon emissions.



Citation: Puškár, M.; Živčák, J.; Lavčák, M.; Šoltésová, M.; Kopas, M. Analysis of Combustion Conditions for Sustainable Dual-Fuel Mixtures. *Sustainability* **2022**, *14*, 13962. <https://doi.org/10.3390/su142113962>

Academic Editors: Karol Tucki and Olga Orynych

Received: 9 October 2022

Accepted: 24 October 2022

Published: 27 October 2022

Publisher's Note: MDPI stays neutral with regard to jurisdictional claims in published maps and institutional affiliations.



Copyright: © 2022 by the authors. Licensee MDPI, Basel, Switzerland. This article is an open access article distributed under the terms and conditions of the Creative Commons Attribution (CC BY) license (<https://creativecommons.org/licenses/by/4.0/>).

Keywords: sustainable; mixtures; combustion

1. Introduction

The limited sources of oil, together with worries over global warming, have increased interest relating to the alternative fuels that can be used in piston combustion engines installed in vehicles [1–5]. The most relevant alternative, which is suitable for heavy commercial and off-road vehicles, is the utilisation of renewable advanced fuels that do not require special adjustments for use in standard diesel engines. In addition to renewable fuels, another possible option is the application of dual-fuel technology; however, this solution requires certain modifications to the currently used concept of diesel engines. In the case of dual-fuel technology, the primary fuel is injected into the engine intake pipe at a low pressure, usually less than 10 bar. This fuel is mixed with the air in order to create a homogeneous fuel–air mixture. This mixture is ignited in the engine cylinder close to the TDC (top dead centre) position through the injection of the ULSDF. While dual-fuel technology is typical for CNG (compressed natural gas) engines, it is also suitable for other alternative fuels. Usually, these kinds of fuels are used to refuel gasoline engine vehicles thanks to their suitable research octane number (RON) value, namely, in the interval $95 \div 110$ [6,7].

In this work, we used an ethanol sustainable mixture (ESM). The maximal ethanol mass portion in the mixture was 85% and the rest of mixture consisted of light gasoline-like hydrocarbons. The main reason for choosing this ESM instead of pure ethanol was because this mixture has already created a network for distribution in a lot of countries; however, pure ethanol, which is used as a fuel in the transport area, is rarely available. This fuel mixture was developed for SI (spark ignition) engines. The main reason for the application of light hydrocarbons concerns the poor flammability characteristics of ethanol in cold engine conditions [8–10]. The research work presented in this article is a continuation of a

previous study performed by Puskar et al. [11,12]. The main task of our scientific-research activities was to investigate how the temperature of intake air influences the combustion of the ULSDF/ESM dual-fuel mixture at various levels of engine load. The performed research focused on the following items:

- Engine operational characteristics;
- Maximal portion of ESM in dual fuel, which corresponds to energy content;
- Engine exhaust emissions.

Despite the number of studies oriented towards the combustion of dual fuels using various fuel combinations and the various investigative approaches applied, there is a lack of relevant information describing dual-fuel combustion. The aim of our scientific-research work was to obtain more information in order to better understand the dependencies of the operational parameters during this kind of combustion process, especially with regard to the application of an ESM as a pre-mixed fuel [13,14].

2. Experimental Analysis

2.1. Test Equipment and Stand

The research experiments performed within this work were realised using a 2.0 L, 4-cylinder TDI (turbocharged direct injection) engine (Table 1) [15]. This piston combustion engine was equipped with a CR system, similar to a basic engine, and another injection system designed to inject ESM into the intake manifold. This additional injection system was made to order. The intake manifold system was also manufactured especially for the purpose of the experiments and structurally arranged so that the individual intake pipes were connected separately to each of the six engine cylinders. The construction of the testing diesel engine and the fuel injection timing were the same as in a standard TDI engine. However, the main time interval of diesel CR injection was reduced in order to keep a constant engine torque when using ethanol as the second fuel. The engine was connected to the dynamometer, which works on the principle of eddy currents and is equipped with a force sensor. Another necessary part of the testing engine equipment was a water–air-type charge air cooler. The temperature of intake air was regulated by changing the cooling-water flow using a valve with manual control.

Table 1. The testing engine data.

Engine	4-Cylinder, CR Injection, Turbocharged
Compression ratio	16.2:1
Bore × stroke	81 × 95.5 mm
Engine volume (displacement)	1968 cm ³
Max rated power output	110 kW
Max engine speed	3500 rpm

The THC (hydrocarbon emissions) were measured using an analyser based on the flame ionization detector principle. Another gas analyser, namely an extractive multi-component gas analyser with a paramagnetic measuring cell, was used to measure the O₂ level. The CO, CO₂ and NO_x emissions were measured with the TEXA analyser and the smoke emissions with the smoke meter. We installed the “Kistler” uncooled piezoelectric sensor on one of the four engine cylinders in order to measure the cylinder pressure values with a 0.5 crank angle (CA) degree. The arrangement of the above-described experimental measuring equipment is illustrated in Figure 1.

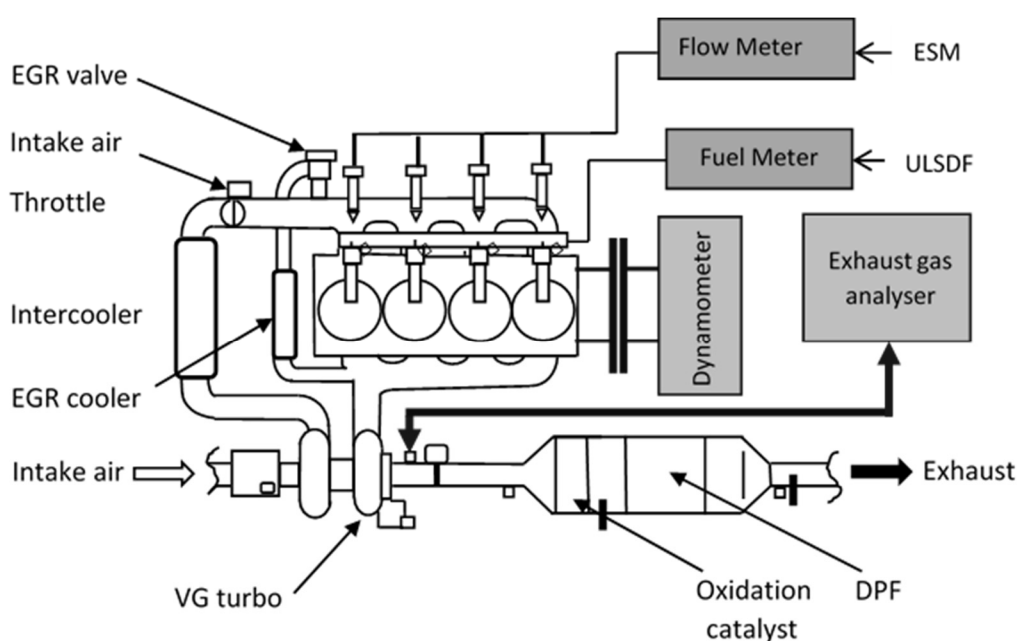


Figure 1. The experimental stand.

The pre-mixed fuel, which was applied in our research work, contained ethanol, whereby the applied analyser was calibrated by the propane, i.e., without oxygen. Therefore, some uncertainties may occur in the values obtained from the THC measurement. Uncertainty regarding the THC measurement depends on the concentration of oxygen-free hydrocarbons and unburned ethanol in the exhaust gases. Taking into consideration the fact that a detailed measurement of the characteristics of HC was not performed in our tests, it is difficult to determine the level of uncertainty in the individual measurements. However, the producer of the above-mentioned analyser promises that the additional error will be less than 1.0%. This error can also be considered as systematic and consistent for all the ESM cases. The engine fuels applied during our tests were commercial fuels: an ESM (85% ethanol) of bioethanol/gasoline and the diesel fuel EN590 (ULSDF) [16–20]. The physical and chemical properties of these tested fuels are presented in Table 2.

Table 2. Properties of the applied fuels.

	ESM	ULSDF
Density, 15 [kg·m ⁻³]	860 ÷ 900	820 ÷ 845
Viscosity (40 °C) [mm ² ·s ⁻¹]	3.5 ÷ 5.0	1.9 ÷ 4.1
Cetane number	min 51	min 47
Sulphur content [mg·kg ⁻¹]	max 10	max 10
Evaporation heat [kJ·kg ⁻¹]	250 ÷ 290	282 ÷ 338
Flash point [°C]	101	82
Carbon content [wt %]	81.5	97.1
Hydrogen content [wt %]	12.1	13.4
Oxygen content [wt %]	10.8	0

2.2. Test Conditions and Methods

We investigated the influence of the intake air temperature under two engine operational conditions (Table 3). The temperature of intake air was reduced from the non-cooled condition to approximately 40 ÷ 50 °C by regulating the water flow through the charge air cooler. The CR injection timing value was maintained at the same level as during the

reference test performed with diesel [21,22]. The reference diesel injection and the testing diesel injection both consist of the pilot injection and the main injection. During the first part of the test, the amount of injected ESM was constant at each load level. The amount of ESM was calculated for both levels of engine load by means of the maximal level of ESM with a PRR value lower than 10 bar/CA under conditions without the cooling of the intake air. The maximal amounts of ESM under conditions of the lowest intake air temperature were investigated in the second phase of the performed test. The pressure value in the engine cylinder was measured for a resolution of 0.25 CA degree. The pressure values obtained from 20 cycles were averaged. This step allowed us to filter out the cylinder pressure fluctuations between the individual cycles. The cylinder pressure data were used in order to determine the heat release rate (HRR). The HRR analysis method, which was used in the given research work, does not take into consideration the evaporation of ESM during compression stroke, exhaust stroke or heat transfer. The exhaust gas emission values were calculated in accordance with the standard ISO, which is determined for the measurement of the gaseous emissions [23–25]. The combustion efficiency of the engine was obtained from the results of the measured CO emissions and THC emissions. The brake thermal efficiency (BTE) was computed as the ratio of the brake output power of the tested engine to the thermal energy delivered to the engine from the fuel.

Table 3. The load and test conditions.

N [rpm]	BMEP [bar]	Intake Air Temp. [°C]	Inlet Air Pressure [bar]	Temperature of Exhaust Gas [°C]	Pressure of Exhaust Gas [bar]
1280	5	90	0.8	395	0.7
	5	70	0.8	368	0.6
	5	60	0.9	355	0.6
	5	50	0.9	348	0.5
	5	40	0.9	332	0.5
	5	30	0.8	330	0.5
1920	10	120	1.0	510	0.9
	10	110	1.0	504	0.9
	10	100	0.9	475	0.9
	10	90	0.8	461	0.9
	10	80	0.8	455	0.9
	10	70	0.8	440	0.8
	10	60	0.8	435	0.8
	10	50	0.8	420	0.8

3. Experimental Results and Discussion

Table 3 presents the boundary conditions which are valid for the individual testing cases. As mentioned above, the temperature of the intake air in the engine load points significantly decreased, while the pressures of intake air and exhaust gas (measured before the turbocharger) remained almost constant [26,27].

The lambda values (λ), which are defined by the intake air mass flow and fuel mass flow, are summarised in Figure 2. These values remained relatively unchanged in both cases of the engine load. A small change occurred for the highest temperature of intake air when applying ESM. Even in the cases of the lowest temperature values, i.e., when the amount of ESM increased, the value of λ moderately changed. If the intake air temperature decreased, the λ values had a moderately increasing trend; however, the individual differences were less than 0.2 [28–34].

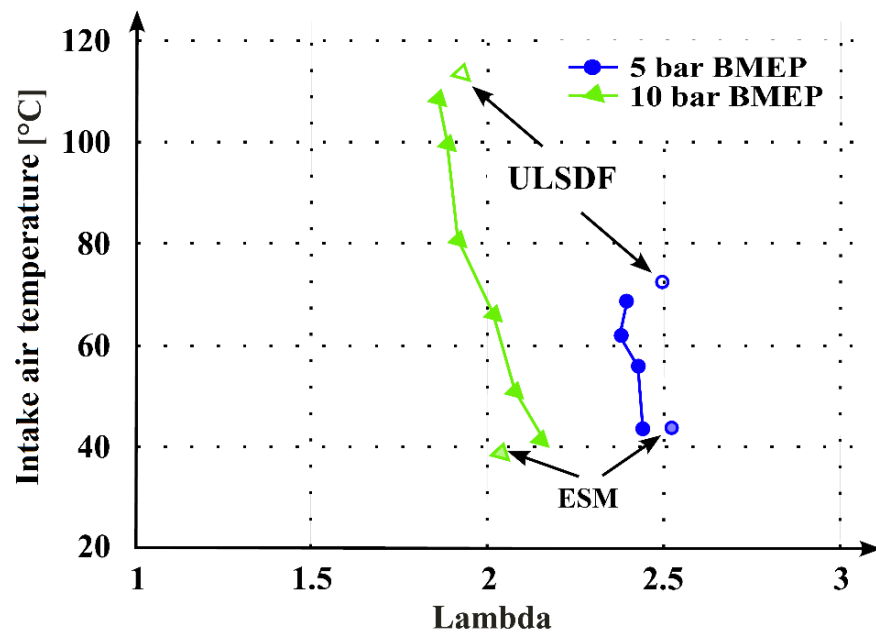


Figure 2. The λ values dependent on air temperatures.

3.1. Pressure in Engine Cylinder and HRR

The cylinder pressures and HRR values at the engine speed of 1280 rpm and at 5 bar BMEP (break mean effective pressure) are visible in Figure 3. The compression pressure values are moderate when using the ESM, which is probably due to the evaporation of fuel during compression stroke. The relevant differences were observed among the maximal cylinder pressure values in the case of different intake air temperatures. In the case of the highest temperature levels, the maximal value of pressure in the cylinder approached the diesel reference value. When the temperature decreased to 50 °C or less, the maximal pressure value also decreased significantly.

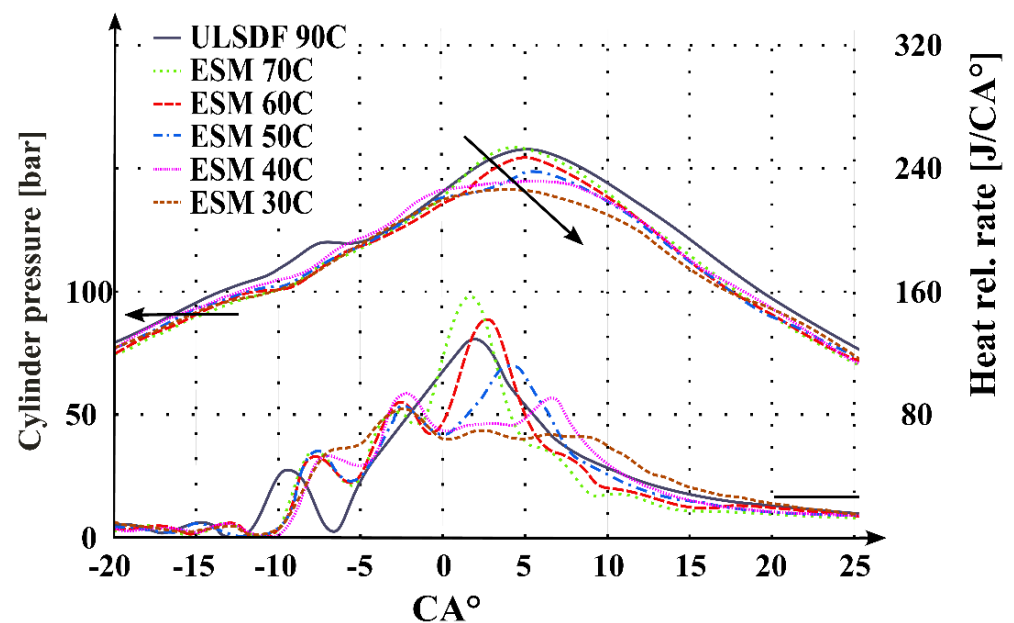


Figure 3. The engine operating characteristics (1280 rpm and 5 bar BMEP).

The HRR data presented in Figure 3 are in good accordance with the values of corresponding pressures in the cylinders. The differences in HRR values and influence of the intake air temperature on ESM combustion after the TDC were even more notable than the

influence on the pressure value curves. It is an evident trend that the peak of HRR is lower and that it occurred later when the intake air temperature decreased. An interesting fact is that the intake air temperature and the amount of ESM at low-level temperatures affected the flame-spread area during the combustion of ESM after the main combustion of diesel. This finding is more remarkable than the ignition delay or combustion of diesel itself.

Figure 4 shows the pressures in the cylinder and the values of HRR at 1920 rpm and at 10 bar BMEP. The temperature of the intake air had a relevant effect on the combustion process at the given load level. There was an evident trend in the self-ignition of ESM at the highest temperature levels. Intake air temperatures below 100 °C changed the behaviour of the combustion process, i.e., there was no detected tendency of self-ignition at these temperatures. Under this operational load, the maximal values of HRR occurred later than the decrease in intake air temperature; however, at 10 bar BMEP, the HRR values increased. This situation can be explained by the increased ignition delay values for the pre-mixed ESM and by the simultaneous usage of the main diesel fuel and the ESM. We observed, in some cases, a phenomenon of three-phase combustion. The first phase was the combustion of pre-injected diesel fuel, the second phase was the combustion of the main diesel fuel after injection of it and the last phase was the combustion of the pre-mixed ESM. This three-phase combustion process was typical, especially when using higher amounts of ESM and at the lowest level of charge air temperature.

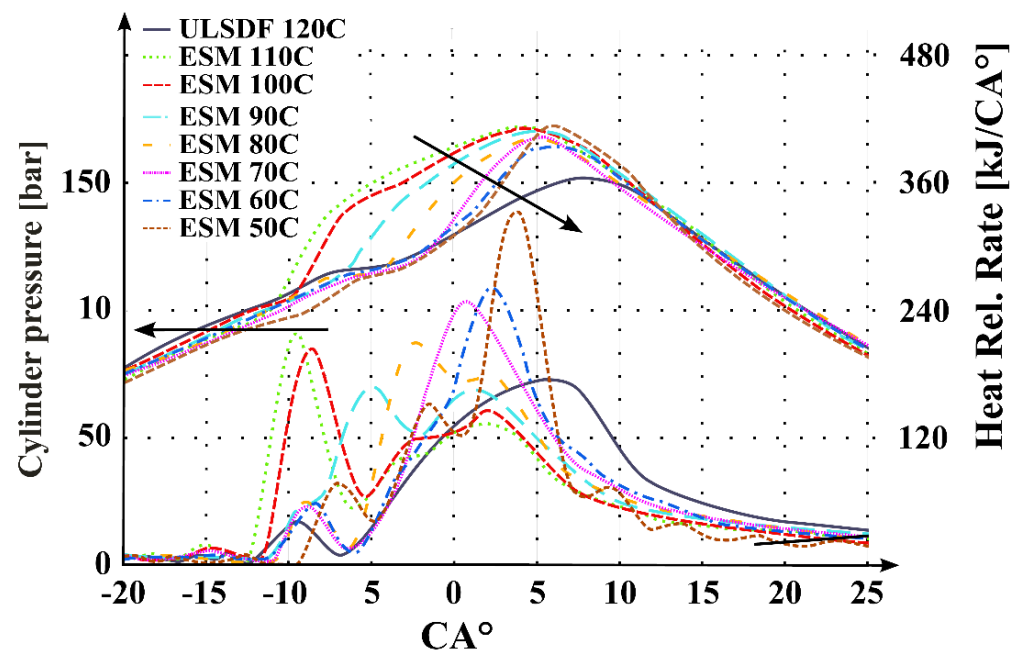


Figure 4. The engine operating characteristics (1920 rpm and 10 bar BMEP).

As mentioned above, it is possible to say that the combustion process in the ESM cases consists of three phases: (1) combustion of pre-injected diesel fuel, (2) combustion of the main injected diesel fuel and (3) combustion of the pre-mixed ESM fuel. This three-phase combustion process was evident in both engine load levels. Excluding the cases of ESM self-ignition, the ignition delay increased when the ESM was used and when the temperature of intake air decreased. The peak values of HRR were higher in the case with ESM. This fact means that only a small amount of ESM was burned in the combustion phase before injection and that the difference in HRR was mainly caused by the increased value of ignition delay. An analysis of diesel fuel combustion after the main injection was more difficult because the combustion of ESM was simultaneous, i.e., during the same time interval. In the case of low engine load, when the ESM combustion was running after the HRR peak values of the main ULSDF combustion, the combustion process analysis was easier. This analysis presented that the ignition of the main charge of diesel fuel was not

significantly affected by the ESM or by the fuel mixture temperature. In the cases of high engine load, the analysis was more demanding because the combustion of ESM occurred before the combustion of the main diesel at charge air temperatures higher than 50 °C, while between temperatures of 50 °C and 40 °C, the combustion of ESM was simultaneous with combustion of the main diesel. The HRR was higher and steeper in the case of ESM, which indicates a high combustion rate in the pre-mixed fuel, as well as the fact that a part of ESM was combusted together with the diesel fuel. The three-peak structure of HRR was evident in the majority of cases, whereby the temperature of intake air had the greatest influence on the ESM combustion. The main reason for the higher dependence was probably a lower reactivity of the fuel mixture, i.e., a low cetane number value and a high temperature of self-ignition compared to diesel (Table 2).

3.2. THC Emissions and CO Emissions

The THC and CO emission values in the tested cases are shown in Figures 5 and 6. Air temperature refers to intake air temp (Table 3). At both load levels, the THC emission values were very close to the zero value in the diesel reference cases. At high-level loads, the decrease in air charge slightly increased the values of the THC emissions, whereby this trend was linear. In the case of the low-level load, the influence of added ESM was higher than in the case of the high-level load. Such a phenomenon was most likely due to a higher amount of ESM at the low load level. At the low load level, the intake air temperature had a very significant effect on the THC emissions because these emissions markedly increased when the temperature of intake air decreased. When the amount of ESM increased in the case of both load levels at the lowest temperature of intake air, the emissions of THC increased. This fact indicates a high rate of unburned fuel.

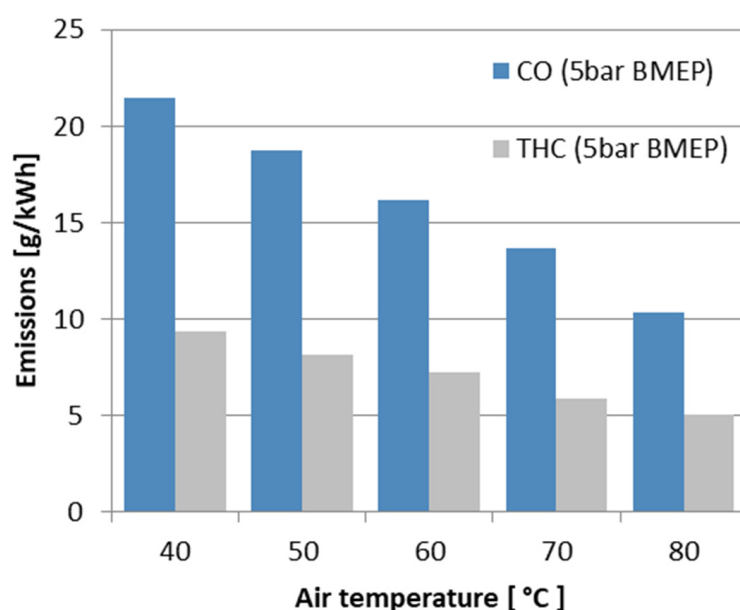


Figure 5. The CO and hydrocarbon (THC) emissions (5 bar BMEP).

With regard to the fact that the THC emissions were considered as an amount indicator of the unburned fuel, the CO emissions indicated the rate of an incomplete fuel combustion process. The main trends were quite similar to those for the THC emissions (Figures 5 and 6), but we also discovered several evident differences. The fuel charge had a stronger and more linear influence on the CO emission values. At the 10 bar BMEP pressure level, the addition of ESM slightly reduced the CO emissions. The emissions of THC and CO increased in all the ESM cases, whereby lowering the intake air temperature tended to increase the amount of emissions, mainly at low loads. In the case of ESM, the THC

and CO emission values were high; therefore, it would probably be necessary to apply an additional post-processing of the exhaust gases in order to fulfil the emission legislation.

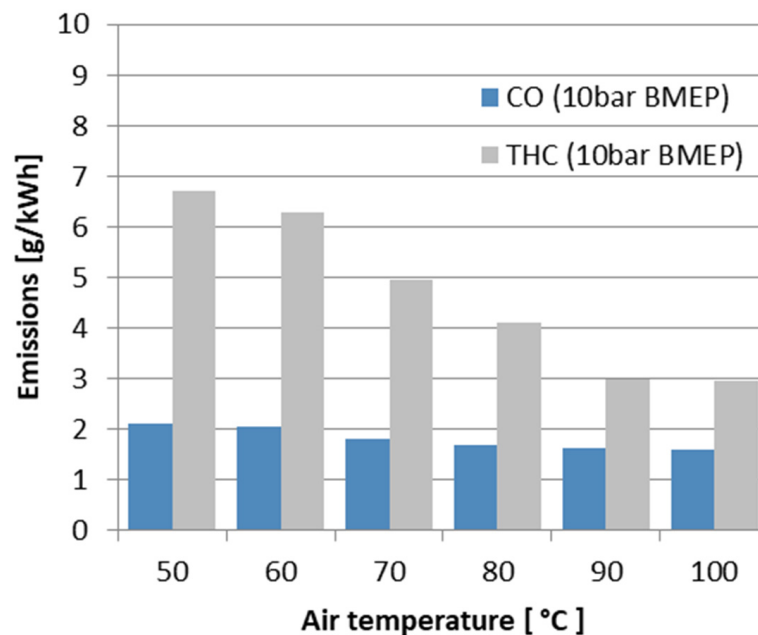


Figure 6. The CO and THC emissions (10 bar BMEP).

The NO_x emissions (Figures 7 and 8) showed an opposing trend compared to the CO and THC emissions. At a low-level load, the addition of ESM to the high temperature charge air reduced the NO_x emissions, while at higher loads, the NO_x emissions moderately increased. Such behaviour can be explained by the tendency for the ESM to self-ignite. One often-mentioned fact is that reductions in the intake air temperature further reduce NO_x emissions in a stable, linear trend. Increasing the ESM portion at the lowest intake air temperature reduces NO_x emissions even further at both engine load levels.

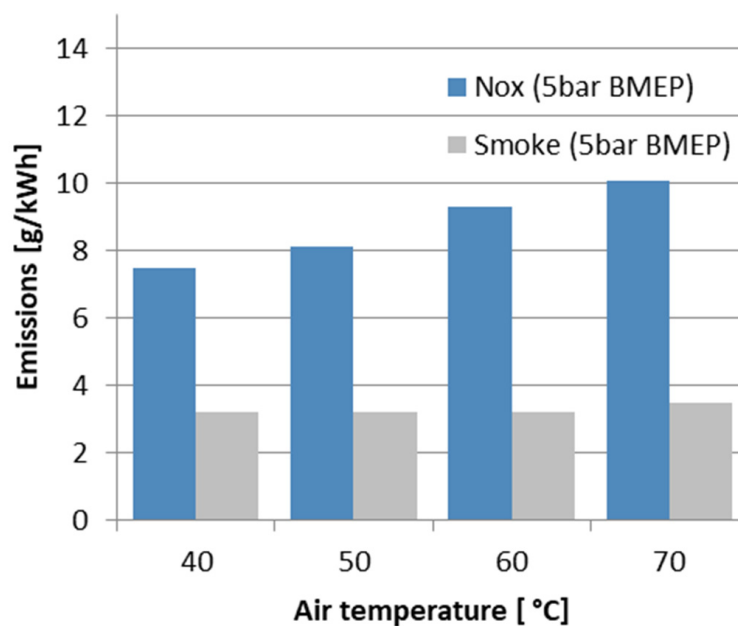


Figure 7. The NO_x emissions (5 bar BMEP).

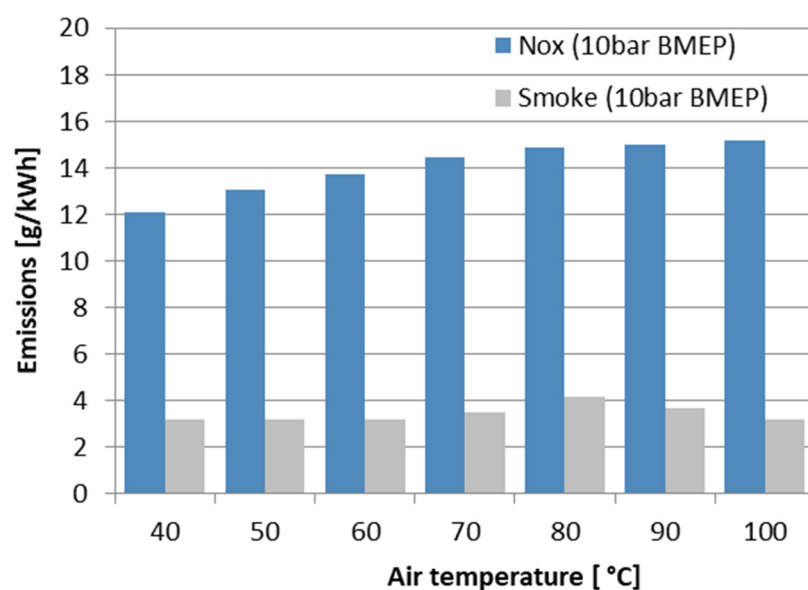


Figure 8. The NO_x emissions (10 bar BMEP).

4. Conclusions

This research work investigated the influence of the charge air temperature on the combustion process of the dual-fuel mixture diesel/ESM. The engine tests were performed at two load levels, namely at 5 and 10 bar BMEP, and using 1280 and 1920 rpm engine speed levels. The portion of ESM for both load levels was given as the maximal portion of ESM in conditions without charge air cooling. At both load levels, we also observed a significantly higher portion of ESM at the lowest temperature of intake air. The amounts of ESM applied in this research work were associated with the energy content, i.e., the portion of ESM in the dual fuel were related to the corresponding energy content.

The main results and conclusions are summarised as follows:

- Reduction in intake air temperature allowed an increase in the acceptable ESM amounts; the highest portions of ESM were approx. 80% at both engine load levels.
- Usage of ESM increased the ignition delay, excepting the case of higher load when ESM was ignited due to self-ignition at high charge air temperature.
- Combustion of the ULSDF/ESM dual-fuel mixture is divided into three parts: (1) combustion of diesel before main injection, (2) combustion of diesel at main injection and (3) combustion of ESM. The temperature of intake air had an important influence on combustion of ESM due to a higher ignition delay at decreasing temperatures.
- The NO_x emissions were reduced using ESM at lower engine loads; however, in the case of higher loads, the trend was opposite. At both load levels, the NO_x emissions were reduced when the charge air temperatures decreased.
- The THC and CO emission trends showed similar growth in the case of both engine loads.
- The presence of ESM and the lower temperature of the charge fuel/air mixture negatively influenced the efficiency of combustion process at both load levels. This was mainly evident at low-level load of 5 bar BMEP, where the efficiency decreased by 10%.

The negative consequences of THC and CO emissions, together with a loss of engine efficiency, can be partially eliminated by optimizing the diesel injection parameters. However, processing the exhaust gases generated during operation of the vehicle piston combustion engines is still unavoidable in order to keep the CO and THC emissions at an acceptable level. This requires a continuation of the presented research within the given subject area and the authors also plan to resolve this issue in future research.

Author Contributions: Conceptualization, M.P. and J.Ž.; methodology, M.P. and M.L.; investigation, M.P. and M.L.; data analysis, M.L. and M.Š.; writing—original draft preparation, M.Š. and M.K.; writing—review and editing, M.K. All authors have read and agreed to the published version of the manuscript.

Funding: This work was supported by the Slovak Research and Development Agency under Contract no. APVV-19-0328. The article was written in the framework of Grant Projects: VEGA 1/0318/21 “Research and development of innovations for more efficient utilization of renewable energy sources and for reduction of the carbon footprint of vehicles” and KEGA 006TUKE-4/2020 “Implementation of Knowledge from Research Focused on Reduction of Motor Vehicle Emissions into the Educational Process”.

Institutional Review Board Statement: Not applicable.

Informed Consent Statement: Not applicable.

Data Availability Statement: Not applicable.

Conflicts of Interest: The authors declare no conflict of interest.

References

- Li, J.; Yang, W.; An, H.; Zhao, D. Effects of fuel ratio and injection timing on gasoline/biodiesel fueled RCCI engine: A modeling study. *Appl. Energy* **2015**, *155*, 59–67. [\[CrossRef\]](#)
- Tucki, K.; Orynych, O. Bioenergy and Biofuels. *Sustainability* **2021**, *13*, 9972. [\[CrossRef\]](#)
- Píštěk, V.; Klimeš, L.; Mauder, T.; Kučera, P. Optimal design of structure in rheological models: An automotive application to dampers with high viscosity silicone fluids. *J. Vibroeng.* **2017**, *19*, 4459–4470. [\[CrossRef\]](#)
- Pušár, M. Advanced System Determined for Utilisation of Sustainable Biofuels in High-Performance Sport Applications. *Sustainability* **2022**, *14*, 6713. [\[CrossRef\]](#)
- Tucki, K. A Computer Tool for Modelling CO₂ Emissions in Driving Cycles for Spark Ignition Engines Powered by Biofuels. *Energies* **2021**, *14*, 1400. [\[CrossRef\]](#)
- Pušár, M.; Živčák, J.; Tarbajovský, P. Complex analysis of combustion and emission parameters of bio-renewable fuel mixtures in dual-fuel mode. *Biofuels Bioprod. Biorefining* **2022**. [\[CrossRef\]](#)
- Pušár, M.; Živčák, J.; Kočíšová, M.; Šoltéssová, M.; Kopas, M. Impact of bio-renewable energy sources on reduction of emission footprint from vehicles. *Biofuels Bioprod. Biorefining* **2021**, *15*, 1385–1394. [\[CrossRef\]](#)
- Toman, R.; Polóni, M.; Chrbík, A. Preliminary study on combustion and overall parameters of syngas fuel mixtures for spark ignition combustion engine. *Acta Polytech.* **2017**, *57*, 38–48. [\[CrossRef\]](#)
- Lamas, M.I.; Rodríguez, C.G. Numerical model to study the combustion process and emissions in the Wärtsilä 6L 46 four-stroke marine engine. *Polish Marit. Res.* **2013**, *20*, 61–66. [\[CrossRef\]](#)
- Pušár, M.; Kopas, M.; Soltesova, M.; Tarbajovsky, P. Simulation Model of Advanced System for Application of Sustainable Fuels. *Int. J. Simul. Model.* **2022**, *21*, 308–319. [\[CrossRef\]](#)
- Lamas, M.I.; Rodriguez, C.G.; Telmo, J.; Rodriguez, J.D. Numerical analysis emissions from marine engines using alternative fuels. *Polish Marit. Res.* **2015**, *22*, 48–52. [\[CrossRef\]](#)
- Kuric, I.; Klačková, I.; Nikitin, Y.; Zajačko, I.; Cisar, M.; Tucki, K. Analysis of Diagnostic Methods and Energy of Production Systems Drives. *Processes* **2021**, *9*, 843. [\[CrossRef\]](#)
- Nieman, D.; Dempsey, A.; Reitz, R. Heavy-Duty RCCI Operation Using Natural Gas and Diesel. *SAE Int. J. Engines* **2012**, *5*, 270–285. [\[CrossRef\]](#)
- Kakaee, A.; Rahnama, P.; Paykani, A. Influence of fuel composition on combustion and emissions characteristics of natural gas/diesel RCCI engine. *J. Nat. Gas Sci. Eng.* **2015**, *25*, 58–65. [\[CrossRef\]](#)
- Ryan Walker, N.; Wissink, M.; DelVescovo, D.; Reitz, R. Natural Gas for High Load Dual-Fuel Reactivity Controlled Compression Ignition in Heavy-Duty Engines. *J. Energy Resour. Technol.* **2015**, *137*, 042202. [\[CrossRef\]](#)
- Zang, R.; Yao, C. Numerical Study of Combustion and Emission Characteristics of a Diesel/Methanol Dual Fuel (DMDF) Engine. *Energy Fuels* **2015**, *29*, 3963–3971. [\[CrossRef\]](#)
- Kováčik, J.; Nosko, M.; Mináriková, N.; Simančík, F.; Jerz, J. Closed-Cell Powder Metallurgical Aluminium Foams Reinforced with 3 vol.% SiC and 3 vol.% Graphite. *Processes* **2021**, *9*, 2031. [\[CrossRef\]](#)
- Maláková, S.; Pušár, M.; Frankovský, P.; Sivák, S.; Palko, M.; Palko, M. Meshing Stiffness—A Parameter Affecting the Emission of Gearboxes. *Appl. Sci.* **2020**, *10*, 8678. [\[CrossRef\]](#)
- Gopinathan, A.; Jerz, J.; Kováčik, J.; Dvorák, T. Investigation of the relationship between morphology and thermal conductivity of powder metallurgically prepared aluminium foams. *Materials* **2021**, *14*, 3623. [\[CrossRef\]](#)
- Můčka, P.; Granlund, J. Is the Road Quality Still Better? *J. Transp. Eng.* **2012**, *138*, 1520–1529. [\[CrossRef\]](#)
- Můčka, P. Longitudinal Road Profile Spectrum Approximation by Split Straight Lines. *J. Transp. Eng.* **2012**, *138*, 243–251. [\[CrossRef\]](#)

22. Ojstersek, R.; Buchmeister, B. Simulation Based Resource Capacity Planning with Constraints. *Int. J. Simul. Model.* **2021**, *20*, 672–683. [[CrossRef](#)]
23. Puškár, M.; Fabian, M.; Kádárová, J.; Blišťan, P.; Kopas, M. Autonomous vehicle with internal combustion drive based on the homogeneous charge compression ignition technology. *Int. J. Adv. Robot. Syst.* **2017**, *14*, 172988141773689. [[CrossRef](#)]
24. Han, X.; Divekar, P.; Reader, G.; Zheng, M.; Tjong, J. Active Injection Control for Enabling Clean Combustion in Ethanol-Diesel Dual-Fuel Mode. *SAE Int. J. Engines* **2015**, *8*, 890–902. [[CrossRef](#)]
25. Puškár, M.; Kopas, M.; Sabadka, D.; Kliment, M.; Šoltéssová, M. Reduction of the Gaseous Emissions in the Marine Diesel Engine Using Biodiesel Mixtures. *J. Mar. Sci. Eng.* **2020**, *8*, 330. [[CrossRef](#)]
26. Pavlenko, I.; Ivanov, V.; Kuric, I.; Gusak, O.; Liaposhchenko, O. Ensuring Vibration Reliability of Turbopump Units Using Artificial Neural Networks. In *Lecture Notes in Mechanical Engineering*; Springer: Cham, Switzerland, 2019; pp. 165–175.
27. Dempsey, A.; Walker, N.; Reitz, R. Effect of Piston Bowl Geometry on Dual Fuel Reactivity Controlled Compression Ignition (RCCI) in a Light-Duty Engine Operated with Gasoline/Diesel and Methanol/Diesel. *SAE Int. J. Engines* **2013**, *6*, 78–100. [[CrossRef](#)]
28. Novotny, P.; Pistek, V.; Drapal, L.; Svida, D.; Devera, T. Efficient approach for solution of the mechanical losses of the Piston Ring Pack. *Proc. Inst. Mech. Eng. Part D J. Automob. Eng.* **2013**, *227*, 1377–1388. [[CrossRef](#)]
29. Vedharaj, S.; Vallinayagam, R.; Yang, W.; Chou, S.; Chua, K.; Lee, P. Experimental investigation of kapok (*Ceiba pentandra*) oil biodiesel as an alternate fuel for diesel engine. *Energy Convers. Manag.* **2013**, *75*, 773–779. [[CrossRef](#)]
30. Mohsin, R.; Majid, Z.; Shihnan, A.; Nasri, N.; Sharer, Z. Effect of biodiesel blends on engine performance and exhaust emission for diesel dual fuel engine. *Energy Convers. Manag.* **2014**, *88*, 821–828. [[CrossRef](#)]
31. Kučera, P.; Píštěk, V. Virtual prototype of a heavy duty off-road truck driveline in Simulink software. In *Proceeding of International Conference Transport Means 2014*; Transport Means. K. Donelaičio st. 73, LT-44029; Kaunas University of Technology: Kaunas, Lithuania, 2014; pp. 5–8. ISSN 1822-296X.
32. Kuric, I.; Kandra, M.; Klarák, J.; Ivanov, V.; Więcek, D. Visual Product Inspection Based on Deep Learning Methods. In *Lecture Notes in Mechanical Engineering*; Springer: Cham, Switzerland, 2020; pp. 148–156.
33. Lamas Galdo, M.I.; Castro-Santos, L.; Rodriguez Vidal, C.G. Numerical analysis of NOx reduction using ammonia injection and comparison with water injection. *J. Mar. Sci. Eng.* **2020**, *8*, 109. [[CrossRef](#)]
34. Kučera, P.; Píštěk, V.; Prokop, A.; Řehák, K. Measurement of the powertrain torque. In *Proceedings of the 24th International Conference Engineering Mechanics 2018*, Svratka, Czech Republic, 14–17, May 2018; pp. 449–452, ISBN 978-80-86246-88-8.